

Numerical Simulation of Pluvial Inundation Considering Gate Operation

Herman MUSUMARI¹, Nakagawa HAJIME², Kenji KAWAIKE³ and Rocky TALCHABHADEL⁴

Numerical Simulation of Pluvial Inundation Considering Gate Operation

Herman MUSUMARI¹, Nakagawa HAJIME²,
Kenji KAWAIKE³ and Rocky TALCHABHADEL⁴

Abstract

The implementation of river embankments to mitigate fluvial flooding inadvertently impacts on the occurrence of pluvial inundation. Receiving rivers and tributaries are linked by gates whose operation becomes crucial when the water level of the main river rises considerably. This study considered a one-dimensional kinematic wave and dynamic wave model for hills and mountains alongside a two-dimensional inundation model based on unstructured meshes applied to lowland areas. It also took into account the interaction between tributaries and the main channel at the downstream boundary as well as gate operation. This resulted in a more realistic simulation of the pluvial inundation that occurred in July 2018 in Oe Town, Kyoto Prefecture. The simulated results were in good agreement with observed data although they revealed a small underestimation. The risk of not operating the gates (on time) was also investigated. In our case, not operating the gates yielded an increase of 40 cm of inundation depth in comparison to the case where the gates were closed on time. We believe that the developed model can be used to effectively assess the mitigation effect of countermeasures such as pumping stations in the coming days.

Key words : Pluvial inundation, fluvial flood countermeasures, gate operation

¹ Master's Student, Dept. of Civil and Earth Resources Engineering, Kyoto University, Japan

² Prof., Disaster Prevention Research Institute (DPRI), Kyoto University, Japan

³ Assoc. Prof., DPRI, Kyoto University, Japan

⁴ Researcher, DPRI, Kyoto University, Japan

1. INTRODUCTION

Flood-related disasters pose a serious threat in Japan. The mountain-dominated topography and rapid growth of cities have induced over half of the population to settle in flood-prone areas. This high exposure to flood proneness accompanied by local torrential rainfall renders flood disasters a common occurrence in Japan (Kawaike et al., 2018).

In addition, these disasters are likely to increase as a result of the rising issue of climate change affecting the frequency and intensity of rainfall patterns (Dale et al., 2015; Shephard et al., 2014). Recently, extraordinary downpours have

punctuated the period spanning from the end of June to the middle of July 2018 with widespread damage and hundreds of casualties in the western part of Japan. Fig. 1 shows 10 days' cumulated rainfall exceeding in some zones the annual average rainfall of the country.

The dynamism of land use characterized by a significant reduction in pervious area alongside heavy rainfall triggered a rapid increase in the water level at several receiving rivers. Consequences pertaining to this high water level are at least twofold. Firstly, the discharge from tributaries becomes difficult to drain into the main receiving

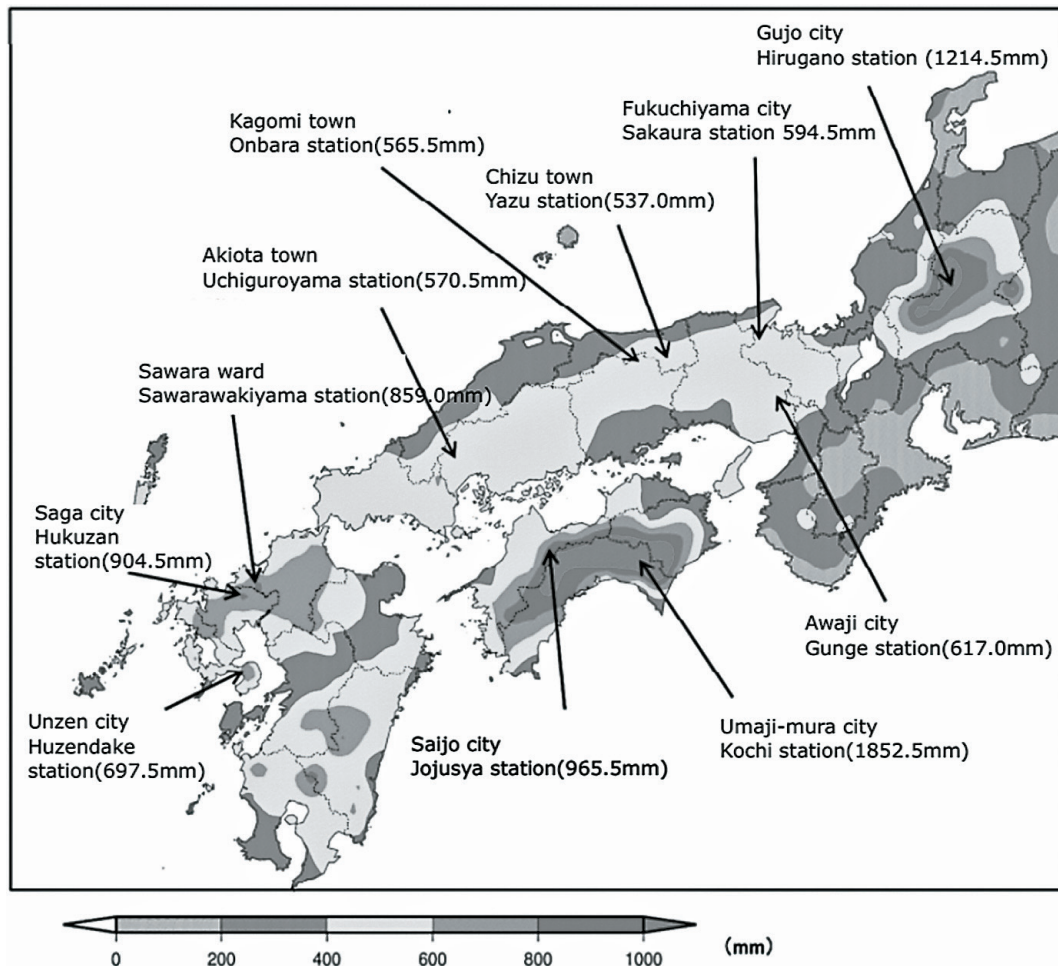


Fig. 1 10 days of rainfall across Japan, July 2018 (Source: Japan Meteorological Agency).

channels. Secondly, the water level of tributaries also rises as a result of the backwater effect, which threatens the stability of contiguous dykes and heightens the risk of fluvial floods by overtopping.

Unlike in Kurashiki City (located in Okayama Prefecture), which witnessed dramatic fluvial inundation due to several levee breaches, serious pluvial inundations occurred in Fukuchiyama City in Kyoto Prefecture and some other cities in Kochi.

While numerous researchers have relied on numerical models to analyze and reproduce flood extension using catchment characteristics, less attention has been devoted to the operation of gates linking the tributaries to the main channels. In fact, although the implementation of embankments aids in reducing the frequency of river overflows, they adversely affect the drainage of the connecting tributaries, especially when the water level becomes sensibly high. Due to this fact, sound flood management requires steady control of the water level on both sides of embankments and the prompt operation of gates in order to resolve the potential backwater effect and avoid the intrusion of discharge from the main rivers that may exacerbate the inundation damage. Gate operation consists of keeping gates open when the water level in the receiving channel is lower in comparison to its tributaries and to shut them when the water level becomes equal or higher.

In order to analyze and reproduce inundation with regard to gate operation, the timing of gate closure is of significant importance. However, the time distribution for the operation of gates is rarely available due to certain policies.

As gate operation directly impacts on the condition of the downstream boundary in the numerical model, our study will focus on different patterns of operation. We will firstly trace back the most likely time of closure based on which pluvial inundation will be reproduced, and secondly investigate the effects of delayed or early gate operation

on flood scale and intensity.

2. STUDY AREA AND DATA

The target area of this study is Oe Town located in Fukuchiyama City on the northwestern side of Kyoto Prefecture. With a total catchment area of 4.9 km² (including the mountainous zone upstream), it is drained by three small rivers flowing into Yura River, a first-class river bending along the city (Fig. 2).

The studied area underwent serious pluvial inundation triggered by two consecutive rainy days (July 6th and 7th of 2018) whose hyetograph provided by AMeDAS at Sakaura station, the closest to our area, is illustrated in Fig. 3. Yura River rose considerably, causing the three gates connecting the Yura to its tributaries to be constrained closed. The importance of pumping stations is recognized in such circumstances to alleviate the inundation and buffer damage by artificially draining water.

Nevertheless, pumps have not yet been implemented in Oe Town. As a result, the small town turned into a reservoir with no outgoing flow discharge.

As shown on the elevation map, Fig. 2, the area is divided into two major parts: the mountainous area from which we estimated the flow discharge, and the lowland area into which the discharge ultimately flowed.

In addition, two essential zones are distinguished within the lowland area: the residential area starting at the toe of the mountains, and the paddy field located between the embankment bearing the railway and the one contiguous to Yura River, Fig. 2.

The former embankment delineates the residential side from the paddy field. Based on this, 34,090 triangular meshes were constructed with an edge size ranging from 1 meter to 10 meters, and five mesh categories were defined to account for river streams, roads, railway, the residential area

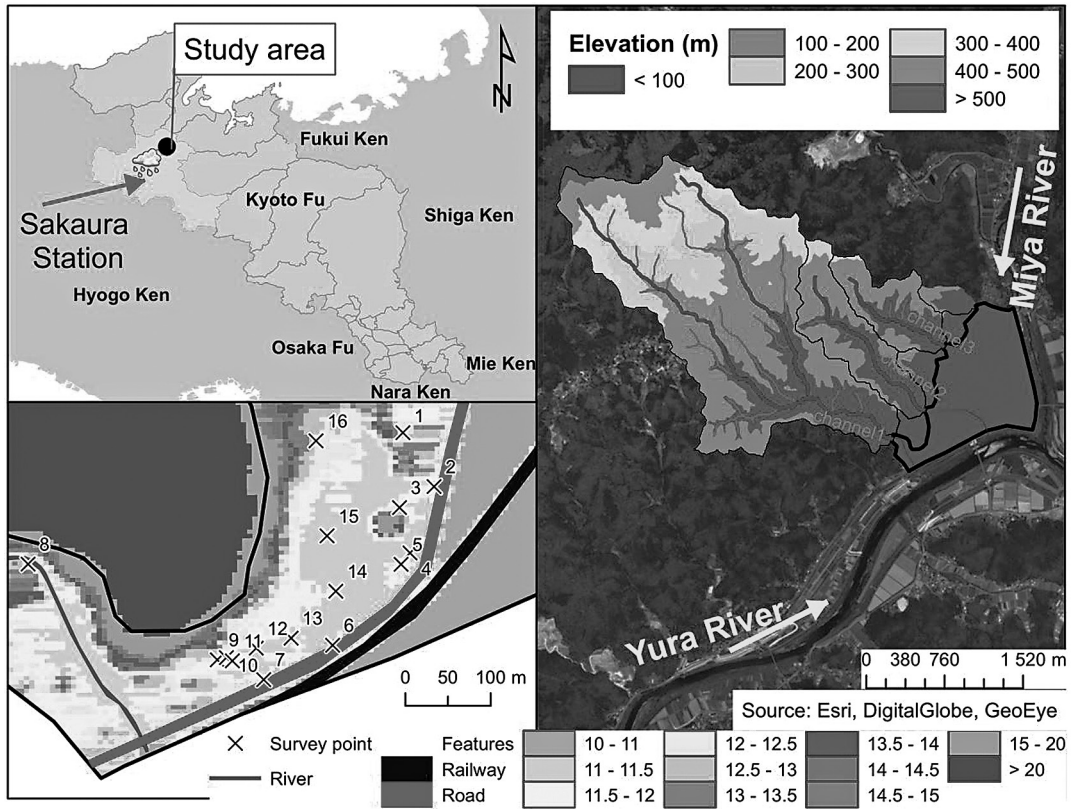


Fig. 2 Target area and the topography of the catchment (including the mountainous area and the inundation zones) provided by 5m x 5m DEM data.

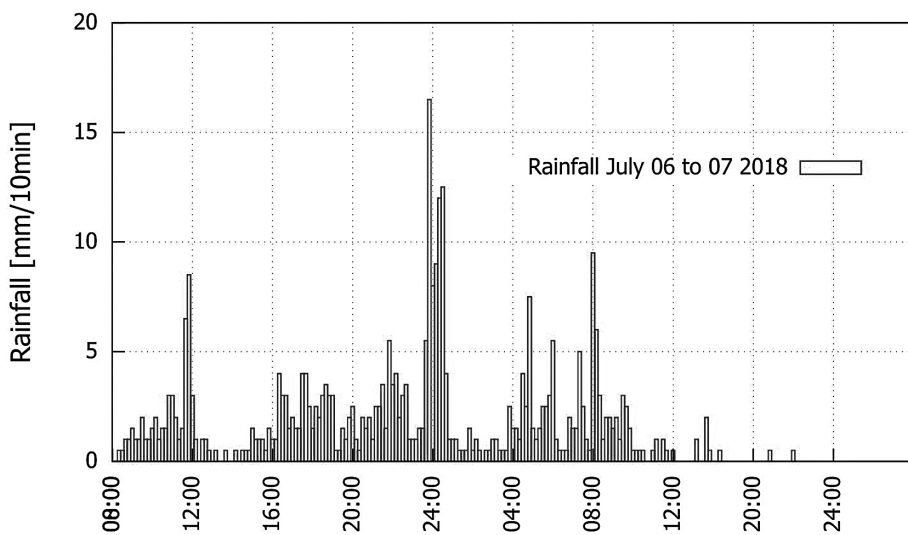


Fig. 3 10 minutes' rainfall distribution observed at Sakaura station.

(with buildings), and paddy field. To each category, a different roughness coefficient was assigned.

3. METHODOLOGY

Numerical methods constitute an essential tool for the depiction and analysis of event-based inundation. Many models, ranging from the simplest conceptual approach to the highly complex physically based models, have been developed and applied to analyze pluvial flooding in many areas throughout the world. In the case of highly urbanized areas with sophisticated channel networks, Lee et al. (2014) applied an integrated model that accounts for the interaction of the sewerage pipe and the overland flow. In contrast, Prasad et al. (2016) focused on pluvial inundation analysis from the perspective of tuning a hazard map with respect to given return periods.

The model used in this paper consists of the conjunction of a 1D kinematic and dynamic wave model with a 2D unstructured mesh model for the inundation propagation applied respectively to the upstream and downstream zones of the target area. To assess the effectiveness of our numerical model in representing the studied event, our team visited Oe Town after the disaster and recorded flood marks at several points (Table 1).

3.1 Numerical model

For the mountainous area, the kinematic wave model and the dynamic wave models have been

applied respectively for slope units, and the main streams. The details are well explained by Takahashi et al. (2001).

The inundation calculation on the downstream area is based on 2D shallow-water equations with the following governing equations:

$$\frac{\partial h}{\partial t} + \frac{\partial M}{\partial x} + \frac{\partial N}{\partial y} = q_{rain}, \tag{1}$$

$$\frac{\partial M}{\partial t} + \beta \frac{\partial uM}{\partial x} + \beta \frac{\partial vM}{\partial y} = -gh \frac{\partial H}{\partial x} - \frac{\tau_{bx}}{\rho}, \tag{2}$$

$$\frac{\partial N}{\partial t} + \beta \frac{\partial uN}{\partial x} + \beta \frac{\partial vN}{\partial y} = -gh \frac{\partial H}{\partial y} - \frac{\tau_{by}}{\rho}, \tag{3}$$

$$\text{With } \frac{\tau_{bx}}{\rho} = \frac{gn^2 u \sqrt{u^2 + v^2}}{h^{1/3}}, \tag{4}$$

$$\frac{\tau_{by}}{\rho} = \frac{gn^2 v \sqrt{u^2 + v^2}}{h^{1/3}}. \tag{5}$$

Here, g is the acceleration due to gravity, u and v are velocities in the x and y directions respectively, $M=uh$ and $N=vh$ represent the flux in the x and y directions respectively, h is the flow depth, ρ is the specific density of water, and β is the momentum correction coefficient. τ_{bx} and τ_{by} are the bottom shear stress along x and y respectively, and q_{rain} designates the source term from the rainfall.

A finite-volume method derived from equations 1, 2, and 3 based on the leapfrog scheme and

Table 1 Observed water depth/level at the residential area

–	Flood Mark	5 m DEM	Water level	–	Flood Mark	5 m DEM	Water level
1	1.60 m	12.50 m	14.10 m	10	2.30 m	12.00 m	14.30 m
2	2.00 m	11.80 m	14.10 m	11	2.20 m	11.80 m	14.00 m
3	1.70 m	12.30 m	14.00 m	12	2.30 m	11.70 m	14.00 m
4	2.60 m	11.40 m	14.00 m	13	2.50 m	11.50 m	14.00 m
5	1.60 m	12.40 m	14.00 m	14	2.60 m	11.40 m	14.00 m
6	2.20 m	11.80 m	14.00 m	15	2.70 m	11.10 m	13.80 m
7	1.80 m	12.10 m	13.90 m	16	1.50 m	12.50 m	14.00 m
8	1.40 m	12.80 m	14.20 m	17	0.60 m	10.80 m	11.40 m
9	2.10 m	12.00 m	14.10 m				

applied to triangular unstructured meshes yields:

$$\frac{h_i^{n+3} - h_i^{n+1}}{2\Delta t} + \frac{1}{A} \sum_{k=1}^3 [M_i^{n+2}(\Delta y)_k - N_i^{n+2}(\Delta x)_k] = q_{rain}, \quad (6)$$

$$\frac{M_L^{n+2} - M_L^n}{2\Delta t} + M_1 + M_2 = -g \left(\frac{d_j h_i + d_i h_j}{d_i + d_j} \right)^{n+1} (\nabla H)_x - T_x, \quad (7)$$

$$\frac{N_L^{n+2} - N_L^n}{2\Delta t} + N_1 + N_2 = -g \left(\frac{d_j h_i + d_i h_j}{d_i + d_j} \right)^{n+1} (\nabla H)_y - T_y. \quad (8)$$

Owing to Fig. 4, M_L and N_L are the x and y flux computed at the middle point of the edge shared by mesh i and j , d_i and d_j are the distance of centroids of mesh i and j to that point, respectively. M_1 and M_2 (resp. N_1 and N_2), which represent the second and third convection terms of the momentum equation, are estimated using the components of the horizontal and vertical flux at the centroid of the computed cell and these fluxes are averaged using the flux at the three edges of the mesh. More details on the formulation of this approach are presented in Kawaike et al. (2000).

3.2 Boundary conditions

The mountainous area was split into a series of rectangular lumped hillslopes in which the rain-

fall was turned into runoff by using a 1D kinematic wave approximation. The outflow discharge of each slope served as a lateral input to the main channels (channel 1, 2, and 3) whose flow routing was computed based on the 1D dynamic wave model. The calibrated Manning coefficients for slopes and river channels were respectively 0.1 and 0.02. The simulated discharge obtained from the mountainous area was thus given as the upstream boundary condition for the inundation modeling (Fig. 5) and the rainfall shown in Fig. 3 is considered as a lateral input for the entire inundation domain.

The basin of channel 2 and 3 being respectively 55474 m² and 66600 m², the two channels exhibit a similar discharge pattern that is highly dependent on their basin's size. The downstream boundary, however, largely depends on the condition at the gates and the subsequent operation. Because of the unavailability of the real operation gates mentioned earlier, Fig. 6 encapsulates different cases considered at the gate boundary, which will allow us to trace back the most likely gate operation and reproduce the inundation event of July 6th to 7th. As the timing of closure is unknown, we run as a first step a simulation by assuming that the water level of Yura River remains lower than the water level of the three tributaries and that the

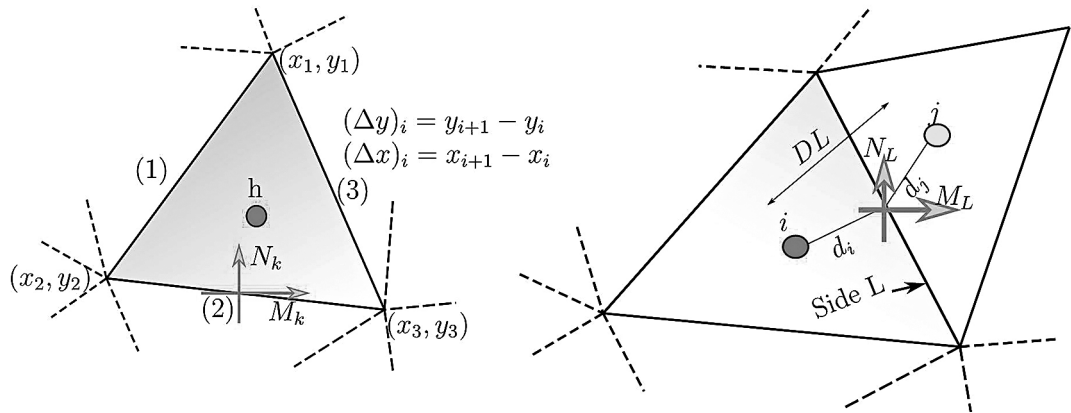


Fig. 4 Control volume (left) and interpolation between meshes (right).

gates stayed open. This first case helps to estimate the theoretical timing of gate operation.

For the second and third case, we embed into the model the interaction between the main river and the tributaries at the gate meshes. Depending on

$$H_Y \leq z_g \Rightarrow q = C_0 \sqrt{2gh_g}, \quad (9)$$

$$z_g < H_Y \leq z_g + h_g \Rightarrow q = \begin{cases} C_1 h_t \sqrt{2gh_g} & \text{if } h_Y / h_g \leq 2/3, \\ C_2 h_d \sqrt{2g(h_g - h_Y)} & \text{if } h_Y / h_g > 2/3, \end{cases} \quad (10)$$

$$z_g + h_g < H_Y \Rightarrow q = \begin{cases} -C_1 h_t \sqrt{2gh_Y} & \text{if } h_g / h_Y \leq 2/3, \\ -C_2 h_d \sqrt{2g(h_Y - h_g)} & \text{if } h_g / h_Y > 2/3. \end{cases} \quad (11)$$

the drainage/overflow discharge exchanged at gates q were computed. Subscripts Y and g refer to Yura River and its tributaries, respectively. H is the water level, h represents the water depth, z the bottom elevation, and $h_t = hg$ and $h_d = \min\{hg, hY\}$. Coefficients $C_0=0.38$, $C_1=0.35$, and $C_2=0.91$ are validated by Kawaike et al. (2018).

Finally, we considered different patterns of the gate operation to represent delayed or early closing in order to assess the impact of these operations on the inundation scale/intensity (focusing on the residential area).

4. RESULTS AND DISCUSSION

Case 1, based on the assumptions that the water level of Yura River remained lower in comparison to its tributaries and that all gates opened throughout the simulation time, revealed that the rainfall of July 6th and 7th, 2018 would not have been enough to trigger inundation if the water level of the main river did not rise significantly as happened on July 6th and 7th, 2018. As illustrated in Fig. 7, the residential area is quasi-non-inundated.

The simulated water level at the gates' meshes from case 1 alongside the observed water level of Yura River allowed us to trace back the theoretical closure timing expressed by the intersection of the two curves (Fig. 8).

This timing at which gates are supposed to be closed to avoid the backwater effect is roughly 12 hours counted from the beginning of the simulation time.

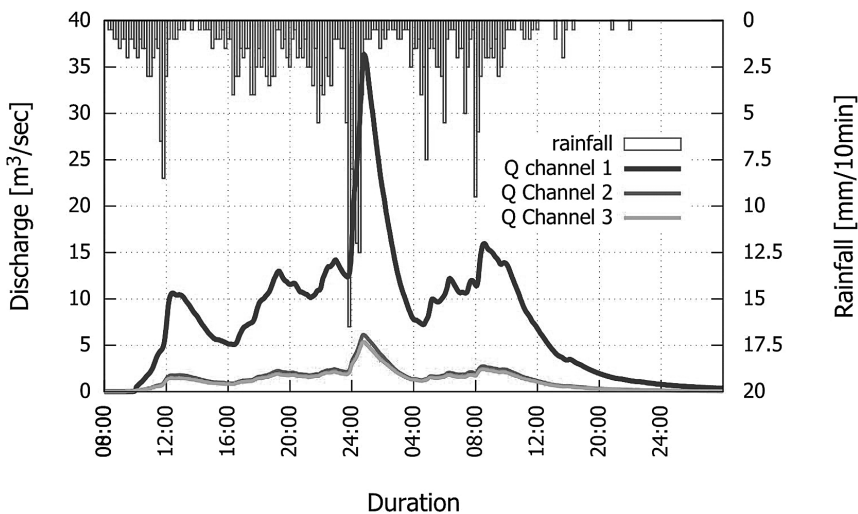


Fig. 5 Discharge given as the upstream boundary condition.

Case 2 served in reproducing the event that occurred in July 2018 and considered the previous timing as well as the interaction between the main river and its tributaries. At time $t=12$ hours, all gates are assumed to shut down simultaneously in

the simulation.

The simulated result is shown in Fig. 9a with a noticeable increase in the flood extent and water depth throughout the domain. There was no significant change in the inundation pattern with respect

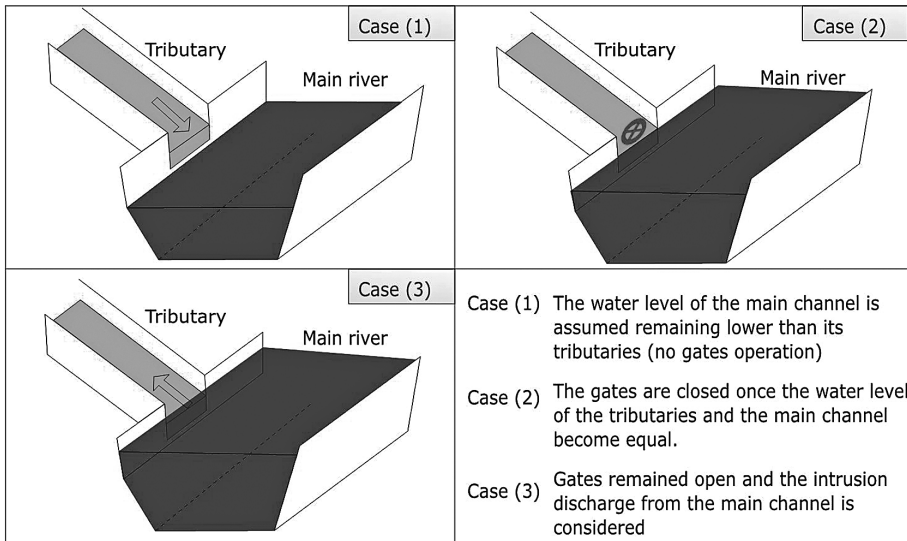


Fig. 6 Schematic representation of different cases.

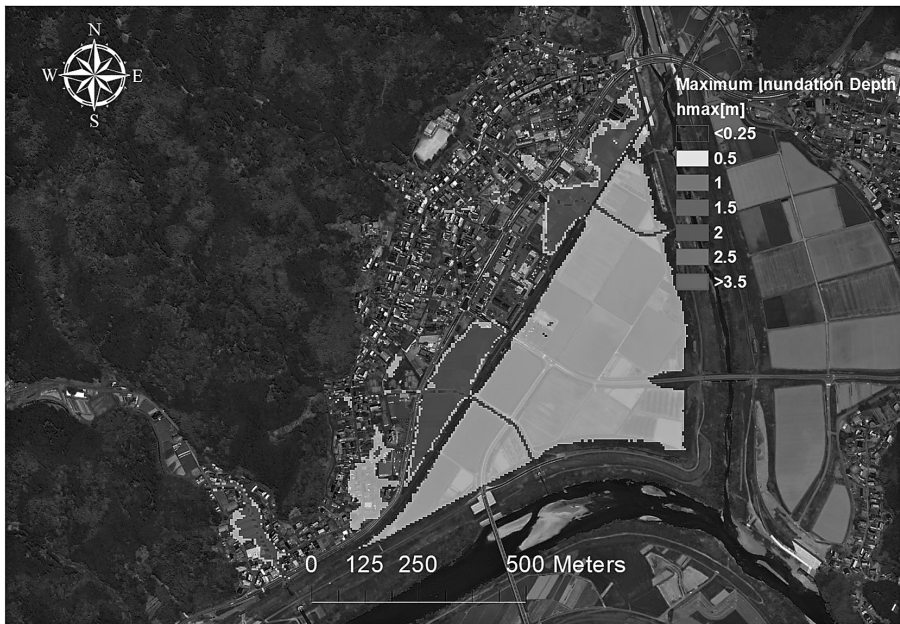


Fig. 7 Inundation distribution from case 1.

to different closure timing for each gate depending on the respective water level time series (not shown here).

A slight underestimation is observed in the set of points (1, 8, 9, 10, 12, 13, and 14) in comparison to the field data (Fig. 9d), and this may be justified by some inaccuracies pertaining to the quality of DEM data. However, the variability is both conserved and reasonable. The inundated domain behaved like a reservoir and the flow progressively

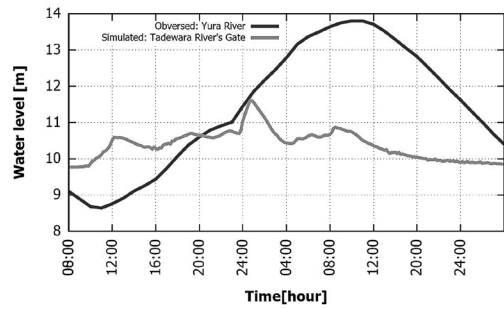


Fig. 8 Water level time series allowing estimation of the closure timing.

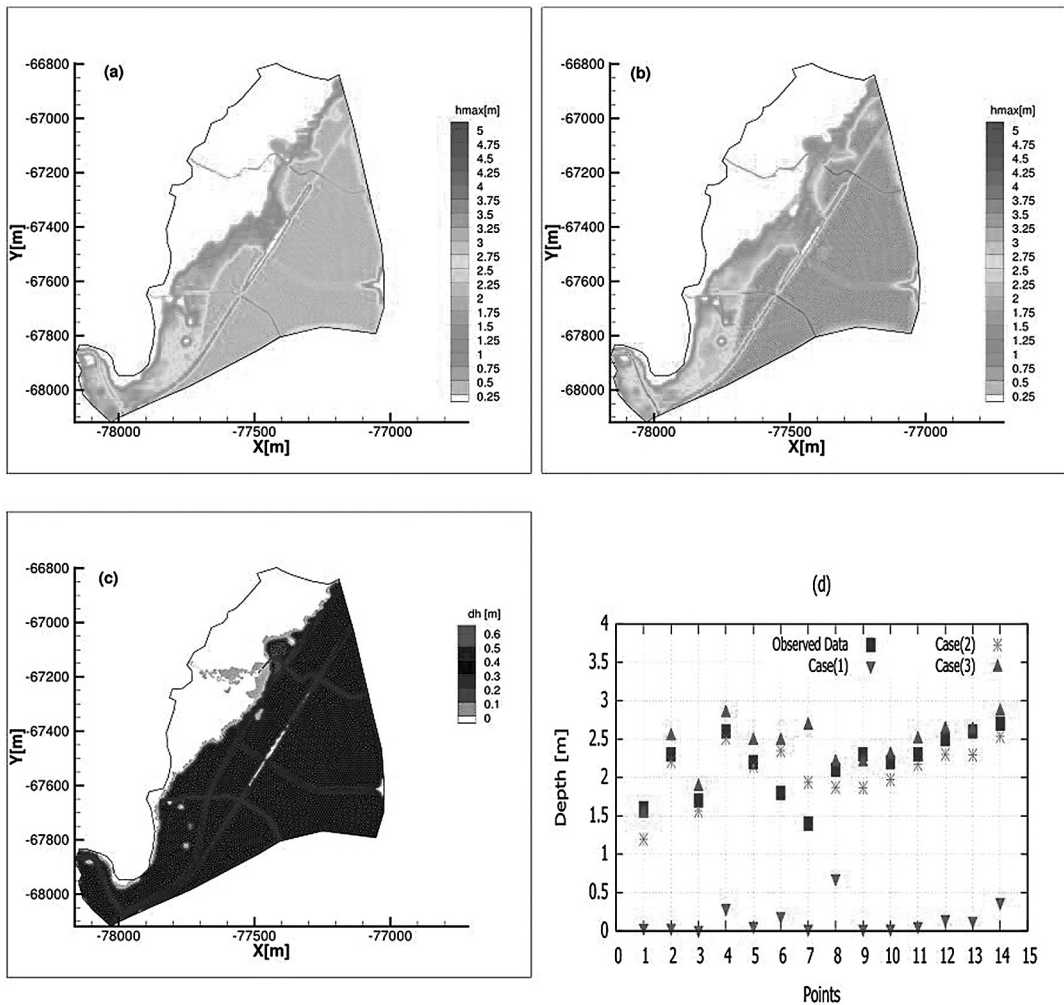


Fig. 9 (a) Case 2 simulation considering the interaction of rivers and the closing time; (b) case 3 simulation considering the interaction of rivers without operating gates; (c) spatial distribution of the difference between case 2 and case 1; (d) comparison between simulated cases and the field data.

filled depression zones as time evolved.

Consequently, the quality of topographical data becomes of utmost importance to precisely assess the water depth throughout the domain and especially in the residential area.

Although the result of case (3) seems close in some points (1, 8, 9, 10, 12, 13, and 14) to the observed data, the root mean square error (RMSE) showed that this case greatly deviated from the reference (field data) with an overestimation trend. The RMSE of case (3) was 0.423, deviating mostly towards high values, while the RMSE of case (2) was 0.3 with a deviation towards lower values. Another explanation behind the underestimation exhibited in case (2) is related to the real timing of closure, which might be greater than the theoretical timing (12 hours) derived from Fig. 8.

$$RMSE = \sqrt{\frac{\sum (\hat{sim} - \hat{obs})^2}{n}} \quad (12)$$

Here, \hat{sim} stands for the simulated values, \hat{obs} designates the observed values, and n is the number of points. When gates are not operated, the flood is more prominent and even significantly exceeds the observed data in some points (5, 6, and 7) as shown in Fig. 9d. The spatial distribution of the difference between case 2 and 3 is shown in Fig.

9c where an increase of 40 cm in both the inundated residential area and the paddy field is noticed. Taking the theoretical closure timing (12 hours) as a reference, two sets of four cases are run. In the first group, gates are closed 1, 2, 3, and 4 hours prior to the reference time. The second group considers the other four cases in which gates are operated after the reference time.

Fig. 10 shows that operating the gates within 4 hours prior to the reference time has similar consequences to not operating them the next 4 hours after that time. An increase in the average inundation depth is noticed when we move away from the reference point, considered here as the theoretical closure timing (12 hours). The gradients of the first and second limb around the reference point are highly dependent on the rainfall pattern and the evolution of the water level in the main river, respectively. However, the sound operation of the gates should intervene as close as possible to the reference time, which corresponds to the minimum inundation depth computed.

5. CONCLUSIONS AND RECOMMENDATIONS

We analyzed a case of pluvial flooding influenced by the conditions at gates joining Yura River

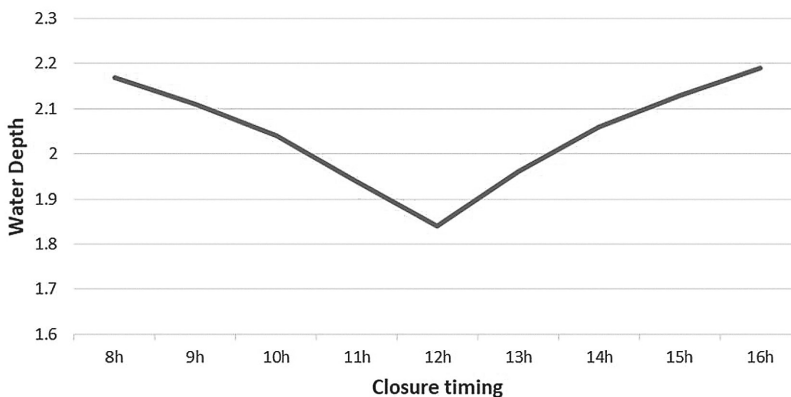


Fig. 10 Average inundation water depth related to different closure timing in the residential area.

with its tributaries. A 1D model for rainfall runoff process and a 2D model for runoff inundation were used in conjunction. The interaction between the main river and its tributaries and the consideration of gate operation allowed us to realistically simulate the inundation intensity as well as the its scale with results that were in good agreement. This study highlighted the importance of operating gates on time, especially when the water level on both sides of the gates becomes equal. Due to the unavailability of the closure timing, we could trace back the most likely time (theoretical time) by combining the observed and the simulated data of the main channel and tributaries, respectively. The results show that delayed interventions resulted in higher inundation depth in comparison to early interventions and that the optimum intervention corresponds to the theoretical closure timing. Future study will incorporate countermeasures such as pumping stations or diversion channels (Niroshinie et al., 2016) into the model and evaluate their effectiveness in the mitigation of damage to a desired level.

References

Dale, M., Luck, B., Fowler, H.J., Blenkinsop, S., Gill, E., Bennett, J., Kendon, E., & Chan, S. (2015). New climate change rainfall estimates for sustainable drainage. *Proceedings of the Institution of Civil En-*

gineers - Engineering Sustainability, 170(4), 214-224.

Kawaike, K., Inoue, K., & Toda, K. (2000). Inundation modeling in urban area based on unstructured meshes. *Hydrosoft, Hydraulic engineering software, WIT Press*, 457-466.

Kawaike, K., Zhang, H., Sawatani, T., & Nakagawa, H. (2018). Modeling of stormwater drainage/overflow processes considering ditches and their related structures. *Journal of Natural Disaster Science*, 39(2), 35-48.

Lee, S., Nakagawa, H., Kawaike, K., & Zhang, H. (2014). Urban inundation simulation incorporating sewerage system without structure effect. *Annals of DPRI, Kyoto Univ.*, 57(B), 407-414.

Niroshinie, M.A.C., Nihei, Y., Ohtsuki, K., & Okada, S. (2016). The countermeasures for flood mitigation evaluated by 1D and 2D coupled models. In *11th ISE*, (pp. 1-5), Melbourne, Australia.

Prasad, J., Kumar, R., & Mani, P. (2016). Combined fluvial and pluvial flood inundation modelling for a project site. *Procedia Technology*, 24, 93-100.

Shephard, M.W., Mekis, E., Morris, R.J., Feng, Y., Zhang, X., Kilcup, K., & Fleetwood, R. (2014). Trends in Canadian short-duration extreme rainfall: Including an intensity-duration-frequency perspective. *Atmosphere - Ocean*, 52(5), 398-417.

Takahashi, T., Nakagawa, H., & Satofuka, Y. (2001). Estimation of debris-flow hydrographs in the Camuri Grande river basin, *Journal of Natural Disaster Science*, 23, 41-50.

(投稿受理：2019年4月5日)

訂正稿受理：2019年7月3日)

要 旨

京都府北部を流れる由良川では、河道からの洪水氾濫対策として本川堤防の整備が進められてきたが、かえってそれが内水氾濫の発生を助長してしまっている。支川とその流下先の本川との合流部には樋門が設置されており、本川水位が上昇した際にはこの樋門の操作が極めて重要になる。本研究では、上流山地部で1次元モデルを考慮し、さらに下流低平地部では2次元氾濫モデルを適用した解析を行った。また、下流端境界においては、樋門操作とともに支川と本川の水位による相互作用を考慮した。このモデルを用いることで、平成30年7月豪雨において福知山市大江町で発生した内水氾濫をより現実的に即してシミュレーションすることができた。解析結果は、やや過小評価になったものの、実測データとよく一致した。さらに本研究では、樋門操作を(適切なタイミングで)行わないリスクについても検討した。解析によると、適切な

タイミングで樋門を閉鎖した場合に比較して、樋門を閉鎖しなかった場合には浸水深が40 cm 大きくなる結果となった。本モデルは、ポンプ設置などの将来的な浸水軽減対策の効果を評価するのに用いることも可能であると考えられる。

キーワード：内水氾濫，門の操作，洪水氾濫対策